

# Synthesis and characterization of lithium holmium silicate solid electrolyte for high temperature lithium batteries

M. Ganesan

Received: 12 March 2008 / Accepted: 12 December 2008 / Published online: 30 December 2008  
© Springer Science+Business Media B.V. 2008

**Abstract** A new Li-ion conducting holmium based solid electrolyte by the sol–gel method was synthesized. The synthesis was carried out at low temperature compared to conventional methods by which lanthanoid silicates are synthesized. The formation temperature of the compound was found through differential thermal analysis and thermogravimetric analysis (DTA-TG). The sintered samples were characterized by X-ray diffraction (XRD), Fourier transform infrared spectroscopy (FTIR), scanning electron microscopy (SEM) and ac impedance spectroscopy. The temperature dependence of conductivity was analysed. The experimental results show that the formation temperature of the lithium holmium silicate was found to be above 500 °C. Highest conductivity obtained was in the order of  $10^{-4}$  S cm<sup>-1</sup> at 750 °C.

**Keywords** Sol–gel chemistry · Solid electrolyte properties · Impedance spectroscopy · Ionic conductivity

## 1 Introduction

There is a growing interest in finding new solid electrolytes for high temperature lithium batteries, which will be useful in military and space applications. Solid electrolytes have many advantages over liquid electrolytes in terms of design flexibility and miniaturization of electronic devices. Commercial development of a solid state lithium battery relies on the successful development of a solid electrolyte with high ionic conductivity. Recently, various types of solid

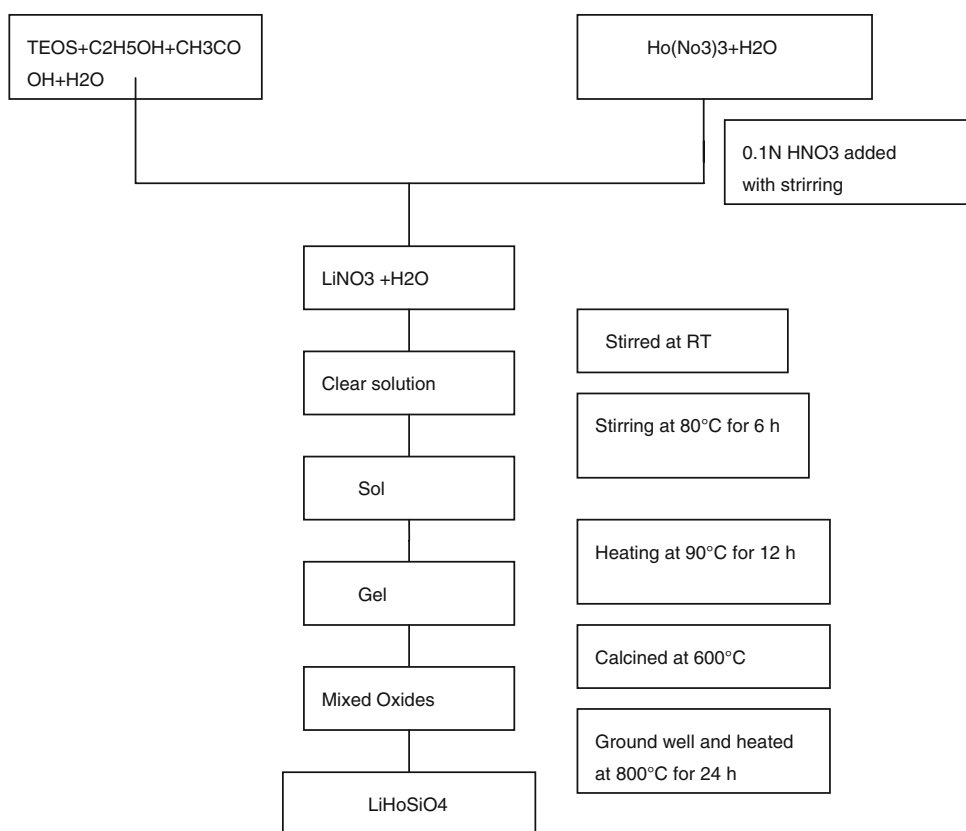
electrolytes for lithium batteries have been found [1–4]. It was reported that lithium lanthanoid silicates exhibit high ionic conductivities at higher temperatures [4]. The conductivity of LiLnSiO<sub>4</sub> prepared by solid-state reaction method with several lanthanoids (Ln = La, Sm, Gd, and Dy) has been reported by Nakayama et al. [5] and Sato et al. [6, 7]. Sato et al. [6] reported the determination of the structure of LiLnSiO<sub>4</sub> and found an apatite structure as a possible solution of the bulk. Many alkali rare earth silicates become high ionic conductors, in which the alkali ions serve as mobile species. Examples include Na<sub>5</sub>YSi<sub>4</sub>O<sub>12</sub> [8], Na<sub>1+x</sub>Zr<sub>2</sub>Si<sub>x</sub>P<sub>3-x</sub>O<sub>12</sub> known as NASICON [9] and Na<sub>3+3x-y</sub>R<sub>1-x</sub>P<sub>y</sub>Si<sub>3-y</sub>O<sub>9</sub> (R = rare earth) known as NARPSIO [10]. Alkali rare earth silicates are particularly suited for an investigation of the relationship between conductivity and structure because of the possibility of very precise tailoring of the crystal lattice, which is constructed by a three-dimensional rigid SiO<sub>4</sub> frame work. For example, mobile species can be replaced by making non-isovalent substitution on the rare earth sites, leaving the silicate frame work structure almost intact. In this communication, for the first time lithium holmium silicate based solid electrolyte with an apatite structure was prepared by the sol–gel method. Through this method, a lower formation temperature was achieved compared to the conventional solid state method. Characterization was done by XRD, FTIR & SEM. The conductivity of the synthesized compound was determined using impedance measurements.

## 2 Experimental

Stoichiometric amounts of lithium nitrate and holmium nitrate were dissolved in nitric acid. This solution was mixed with appropriate amounts of ethanol, acetic acid,

M. Ganesan (✉)  
Electrochemical Energy Systems Division, CECRI,  
Karaikudi 630006, India  
e-mail: mgshan2002@yahoo.co.in

**Fig. 1** Flow chart for the synthesis of  $\text{LiHoSiO}_4$



tetraethoxysilane (TEOS) and water. A clear sol was formed after stirring the mixture at 80 °C for about 6 h. The sol transforms into a gel after heating at 90 °C for 12 h. The precursor compound was analysed by differential thermal analysis and thermogravimetry using a STA 1500 TG/DTA analyser. This gel was calcined at 600 °C for 7 h to get mixed oxides by removing the organic components. The “as calcined” powder was ground well and pure lithium holmium silicate was obtained by further calcining the powder at 800 °C for 24 h. The flow chart for the preparation of  $\text{LiHoSiO}_4$  is given in Fig. 1.

The pure lithium holmium silicate powder obtained after calcining was crushed into fine powder and spread in a die. A pressure around  $4,000 \text{ kg cm}^{-2}$  was applied to form pellets of 0.1 cm thickness and 1.5 cm diameter. These pellets were sintered at 800 °C for 24 h. The sintered samples were characterized using X-ray diffraction (JEOL-JDX 8030 X-ray diffractometer,  $\lambda = 1.5406 \text{ \AA}$  using  $\text{CuK}_\alpha$ ), FTIR (Perkin-Elmer Paragon-500 FTIR spectrophotometer in the region  $400\text{--}4,000 \text{ cm}^{-1}$ ) and scanning electron microscopy (Hitachi S-300 H scanning electron microscope). For impedance measurements an AUTOLAB PGSTAT 30 with FRA was used. An ac amplitude of 5 mV in the frequency range 100 kHz to 1 Hz was used. The pellets were placed between two discs made of gold coated stainless steel and were then placed inside a muffle

furnace for conducting impedance measurements at different temperatures.

### 3 Results and discussion

#### 3.1 TG/DTA

To understand the formation temperature of the compound, as well as changes occurring during formation such as decomposition of the organic components, phase formation and transition temperature, the precursor sample of the compound was subjected to thermal analysis and the results are shown in Fig. 2. The formation of the compound follows three steps. First region (from 30 to 210 °C) shows 35% weight loss of the sample, which accounts for the entrapped moisture inside the precursor. The second region (from 210 to 310 °C) with a weight loss of 20%, corresponds to the decomposition of organics. The third region (from 310 to 536 °C) reflects a the weight loss of 13%, which may be due to the decomposition of nitrates and other components. There is no weight loss after 536.03 °C indicating the completion of the reaction thus leading to the formation of the compound at this temperature.

The DTA data shown in Fig. 2 for the sol–gel product with Li:Ho ratio of 1:1, indicates the highest exo effect at

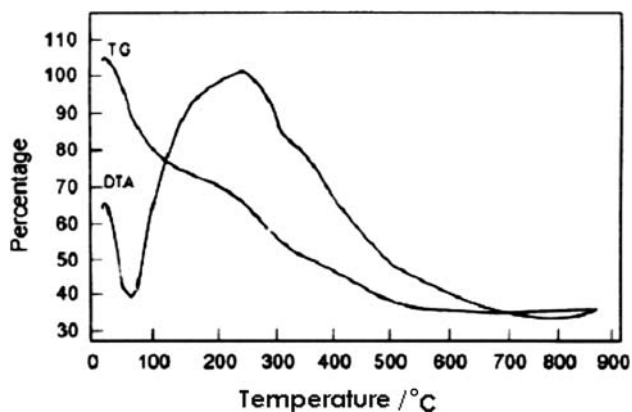


Fig. 2 TG/DTA for LiHoSiO<sub>4</sub>

250 °C due to the decomposition of organics which corresponds to the mass loss in the sample occurs at 250–536 °C in thermogravimetric analysis. The resultant product formed at low temperature tends to create large defects with grain and grain boundaries which are responsible for lithium ion conduction.

### 3.2 XRD

X-ray diffraction analysis was carried out to confirm the formation of LiHoSiO<sub>4</sub>. As shown in Fig. 3 X-ray diffraction pattern for LiHoSiO<sub>4</sub> displays characteristic peaks at  $2\theta = 23.7^\circ$ ,  $27.7^\circ$  and at  $33.3^\circ$  with d spacing of 3.175 Å, 3.218 Å and 2.668 Å. This pattern is well matched with the XRD patterns of apatite structure of LiLnSiO<sub>4</sub> (Ln = Lanthanoid) as reported earlier [5]. Matsumoto et al. [4] reported a sharp and characteristic peak around  $2\theta = 30^\circ$  which corresponds to maximum orientation of grains at the 211 plane for LiLaSiO<sub>4</sub>. This is shifted towards higher angles here as the ionic radius of the Holmium is less compared to that of Lanthanum.

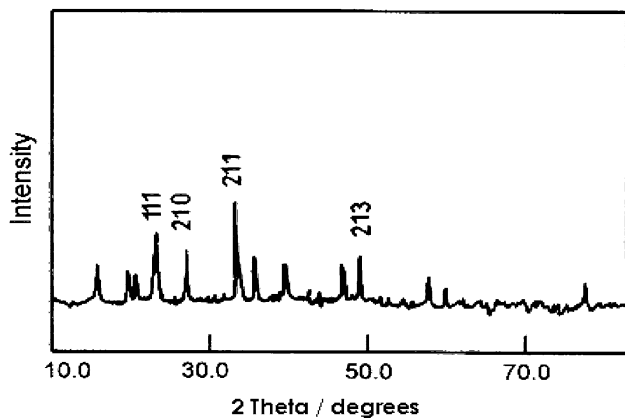


Fig. 3 XRD for LiHoSiO<sub>4</sub>

### 3.3 FTIR

Figure 4a shows the FTIR spectra for the precursor (LiOH, Ho(NO<sub>3</sub>)<sub>2</sub> & TEOS) material heated to 90 °C. The broad bands in the regions 3,200–3,400 cm<sup>-1</sup> and at 1,630–1,650 cm<sup>-1</sup> may be attributed to stretching and bending vibrational modes of the O–H of molecular water and the Si–OH stretching of surface silanol hydrogen bonded to molecular water. The band in the 1,350–1,475 cm<sup>-1</sup> region corresponds to Ho–O asymmetric stretching vibration in HoO<sub>3</sub> units. The band in the region 910–925 cm<sup>-1</sup> is assigned to Ho–O bond vibration of HoO<sub>4</sub> units. The broad band at 1,100–990 and 750 cm<sup>-1</sup> may be due to the stretching mode of broken Si–O bridges. The band at 475 cm<sup>-1</sup> corresponds to the deformation mode of Si–O–Si [11].

Figure 4b shows the FTIR spectra of the synthesized LiHoSiO<sub>4</sub>. The spectra show the disappearance of a band at 1,100 cm<sup>-1</sup> and appearance of a band at 940–999 cm<sup>-1</sup>, which is associated with the formation of a ring structure of SiO<sub>4</sub> tetrahedral [12] as well as the stretching frequency of Si–O–Ho and it is especially significant in crystalline phase. A band at 1,440–1,485 cm<sup>-1</sup> is attributed to the

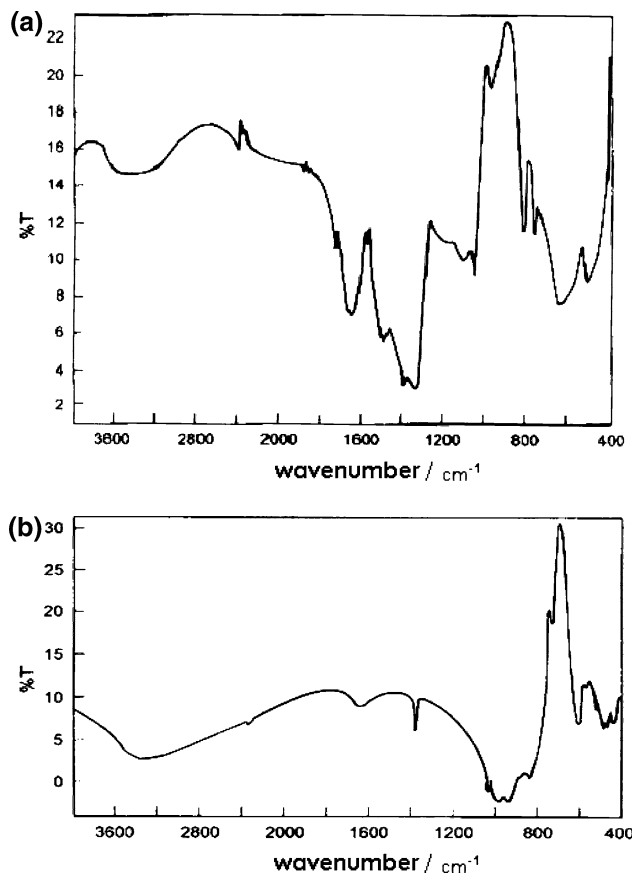


Fig. 4 FTIR for LiHoSiO<sub>4</sub> at (a) 90 °C (b) 800 °C

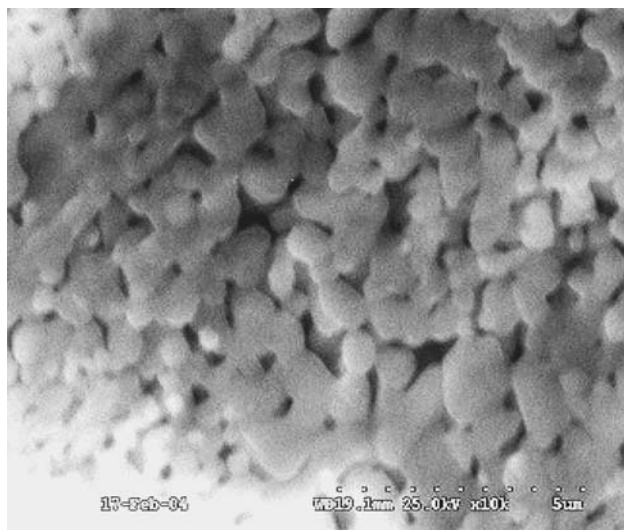


Fig. 5 SEM for LiHoSiO<sub>4</sub>

formation of a Holmium–silicate linkage. The crystalline phase formation is confirmed from XRD results.

3.4 SEM

Figure 5 shows the SEM for the sample LiHoSiO<sub>4</sub> pellet. Particles of the order of 5–10 μm are evenly distributed over the surface. Grains are oriented randomly with well defined inter-grain contact.

3.5 Impedance analysis

Figure 6 shows the typical complex impedance diagrams obtained at different temperatures viz at 600–750 °C for the specimen sintered at 800 °C. At temperatures 600 and 650 °C two semicircles are observed. The one at high frequency is due to the response of the grains and the other at low frequency is attributed to grain boundaries. Grain conduction is required in preference to grain boundary conduction for lithium ion conducting material to be operated at high temperatures.

At temperatures 700 and 750 °C, a single semicircle is obtained which is due to the grains. As the temperature increases, inter-grain contact resistance becomes smaller due to grain reorientation. This may also be due to agglomeration of the grains where the grain boundary vanishes. As the temperature is increased the enhancement of conductivity is seen by the reduction in the diameter of the circular arc which is due to disappearance of grain boundaries.

The Equivalent circuit is assumed as described in Fig. 7 and this is conceived as resistors and capacitors due to grain and grain boundaries of the specimen placed between two blocking electrodes. The contribution towards the

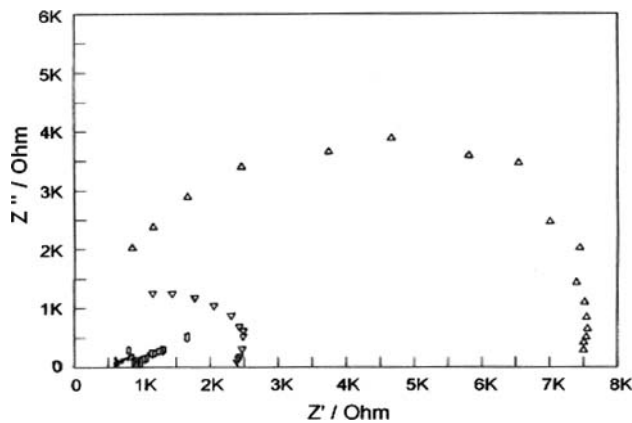


Fig. 6 Impedance spectroscopy at few temperatures

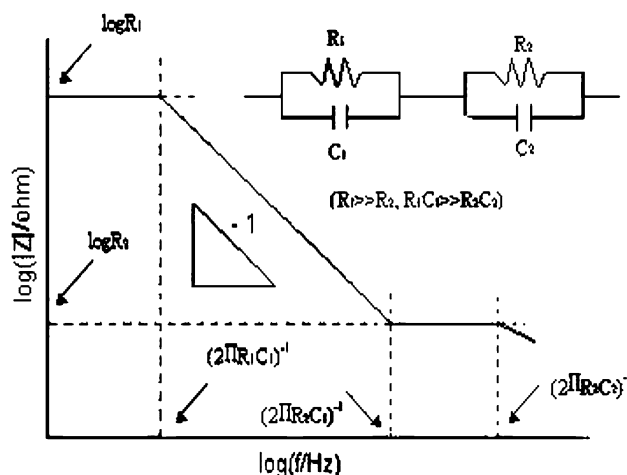


Fig. 7 Equivalent circuit diagram

Table 1 Values of solution resistance (R<sub>1</sub>) and polarisation resistance (R<sub>2</sub>) for the synthesized LiHoSiO<sub>4</sub>

Temperature (°C)	R <sub>1</sub> (ohm)	R <sub>2</sub> (ohm)
600	1.8825 × 10 <sup>2</sup>	4.9949 × 10 <sup>4</sup>
650	2.4090 × 10 <sup>3</sup>	1.6021 × 10 <sup>4</sup>
700	2.9731 × 10 <sup>3</sup>	4.7915 × 10 <sup>2</sup>
750	1.6985 × 10 <sup>3</sup>	3.092 × 10 <sup>2</sup>

leads and electrode contact resistances are attributed to R<sub>1</sub> (ohmic resistance) and that of resistance due to grains and grain boundary are attributed to R<sub>2</sub> (Polarisation resistance). These values are calculated and tabulated in Table 1. The capacitance due to grain and grain boundaries are represented as C<sub>1</sub> and C<sub>2</sub>. As discussed earlier, as the temperature is increased, capacitance due to grain boundary vanishes and only capacitance and resistances (C<sub>1</sub> and R<sub>2</sub>) due to grains exists. The polarisation resistance decreases as the temperature is increased, thus leading to enhanced conductivity of the order of 10<sup>-4</sup> S cm<sup>-1</sup>.

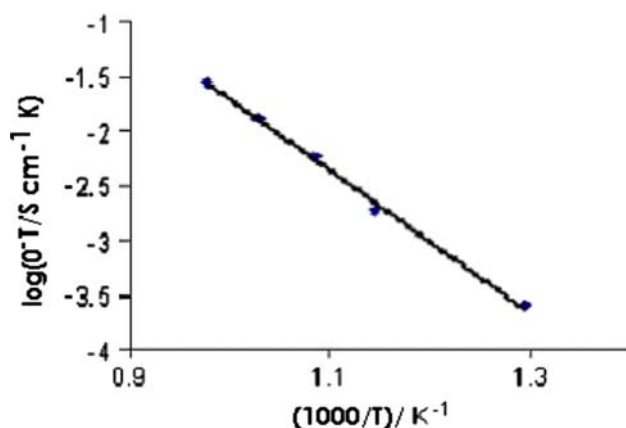


Fig. 8 Temperature dependency of conductivities for LiHoSiO<sub>4</sub>

### 3.6 Temperature dependency of conductivity

Conductivities are calculated from the resistances obtained from the impedance plots. Conductivity increases with increase in temperature. Conductivities obtained at different temperatures are parameterised by the Arrhenius equation

$$\sigma = \sigma_0 \exp(-E_a/kT)$$

where  $\sigma$  is the conductivity and  $\sigma_0$  is the pre exponential factor.  $E_a$  is the activation energy,  $k$  is the Boltzmann constant and  $T$  is absolute temperature, respectively. The temperature dependency of the conductivities is shown in Fig. 8. From the  $\log(\sigma T)$  vs  $1000/T$  plot, activation energy was calculated and the value obtained is 0.5 eV. The obtained value is better than that reported for lanthanum silicate (0.64 eV) [13].

## 4 Conclusion

Lithium holmium silicate solid electrolyte was prepared by the sol–gel method for the first time. Easy preparation, low

processing temperature, phase purity, better size and morphological control are some of the advantages of this method. From the experimental results it is concluded that the sintered sample exhibits fairly high conductivities at higher temperatures. The highest conductivity obtained using this method is in the order of  $10^{-4}$  S cm<sup>-1</sup> at 750 °C. The activation energy obtained for this sample was 0.5 eV.

**Acknowledgments** The author thanks the Director, CECRI for his kind permission to publish this article and also thank DRDO for their financial support for the work.

## References

1. Basu B, Sundaram SK, Maiti HS, Paul A (1986) Solid State Ionics 21:231–238
2. Saito Y, Asai T, Ado K, Kageyama H, Nakamura O (1990) Solid State Ionics 40/41:34–37
3. Chen RF, Song XQ (2003) Hebei shifan Daxue Xuebao, Ziran Kexue ban 27(1):56–59 (ch)
4. Matsumoto H, Yonezawa K, Iwahara H (1998) Solid State Ionics 113–115:79–87
5. Nakayama S, Sakamoto M (1992) J Ceram Soc Jpn 100:867
6. Sato M, Kono Y, Uematsu K (1994) Chem Lett 23:1425
7. Sato M, Kono Y, Ueda H, Uematsu K, Toda K (1996) Solid State Ionics 83:249
8. Shannon RD, Tayler BE, Gier TE, Chen HY, Berzins T (1978) Inorg Chem 17:958
9. Goodenough JB, Hong HYP, Kafalas JA (1976) Mater Res Bull 11:203
10. Yamashita K, Nojini T, Umegaki T, Kanazawa T (1989) Solid State Ionics 35:299
11. Nakamoto K (1997) Infrared and Raman spectra of inorganic and coordination bonds, 5th edn. Wiley, p 163
12. Colthup NB, Daly LH, Wiberley SE (1964) Introduction to infrared and Raman spectroscopy. Academic Press, New York
13. Tao Shanwen, Irvine John TS (2001) Mater Res Bull 36:1245–1258